https://doi.org/10.5194/egusphere-2024-3093
Preprint. Discussion started: 27 November 2024


# Regional transport of aerosols from Northern India and its impact on boundary layer dynamics and air quality over Chennai, a coastal megacity in Southern India.

Saleem Ali[1], Chandan Sarangi[1*] and Sanjay Kumar Mehta[2]

[1]Department of Civil Engineering, Indian Institute of Technology Madras, Chennai, 600036, India
[2]Atmospheric Observations and Modelling Laboratory (AOML), Department of Physics and Nanotechnology, SRM Institute of Science and Technology, Kattankulathur, 603203, India
*Correspondence to*: Chandan Sarangi (chandansarangi@civil.iitm.ac.in)

**Abstract.** Westerly driven regional transport of aerosols from the heavily polluted North India towards south-eastern India is a prevalent phenomenon during the winter season. Here, the regional aerosol transport events on the boundary layer dynamics and air quality over Chennai, a tropical South Asian megacity, are investigated. The long-term satellite data enables us to depict such regional transport events prolonged for a few days, accounting for ~10-13 per cent of the winter season. The occurrence of these regional transport events is increasing over time in southeastern India which are associated with relatively calmer conditions under anticyclonic wind circulation over north India extending to south India. The transported aerosol layer is generally located around ~1-3 km across the entire southeastern India, capped by the strong atmospheric temperature inversion. The regional aerosol/ haze transport significantly reduces the boundary layer height (ABL-H) by ~38% compared to clear sky conditions ( ~2-2.5 km). Consequently, an increase in $PM_{2.5}$ is observed to be ~30-35% in association with the strong heating aloft ABL (~1.2-2.5K), suppression of ABL-H and anticyclonic circulation over north India. This study provides robust observational evidence on the importance of regional transport of aerosols on air quality of downwind megacities and warrants more observational and modelling studies to constrain the inherent aerosol-induced effects on boundary layer dynamics.

## 1. Introduction

Atmospheric aerosols are pivotal in regulating Earth's climate systems by influencing radiation budget, cloud properties and biochemical cycles. Direct and indirect effects of aerosols on the radiation balance of the Earth-Atmosphere system are evident (Comstock and Sassen, 2001; Haywood and Boucher, 2000; Lohmann and Feichter, 2005; Satheesh and Krishnamoorthy, 2005; Yu et al., 2006) and it is believed to generate climate perturbations on a regional and global scale. Apart from the local generation, the long-range transport of aerosols from their sources can severely pollute a large area far from the apportionment and it is mainly influenced by the atmospheric circulation and aerosol lifetime. Although local emissions contribute mainly to hazy episodes in megacities, it can also be influenced by regional pollutant transports (Ma et al., 2020; Mhawish et al., 2022). Such hazy events can cause severe air pollution, adversely affecting public health. Prolonged haze events and associated high $PM_{2.5}$ loading have frequently been reported over South Asia and China during recent autumn and winter seasons (Qin et al., 2016; Yang et al., 2020; Zhang et al., 2021a). The significant factors influencing such hazy events were attributed to stable synoptic conditions with weak surface winds and low Atmospheric Boundary

https://doi.org/10.5194/egusphere-2024-3093
Preprint. Discussion started: 27 November 2024


Layer (ABL) height (Wang et al., 2014) along with the regional aerosol transport and ABL interaction (Zhang et al., 2015).

Such transported aerosol layers, stratified above the ABL, can significantly affect the surface energy balance and ABL dynamics owing to their interaction with incoming solar radiation (Ding et al., 2016; Ma et al., 2020). Depending on the dominant aerosol species, the net impact of these layers could be absorbing or scattering of incoming solar radiation. In either case, the presence of this transported aerosol layer can induce cooling at altitudes below the layer and warming around and above the altitudes where they are located. Simultaneously, near-surface accumulation of absorption aerosol concentration (under a shallower boundary layer) can lead to lower atmosphere warming and surface cooling. Thus, a series of thermodynamical effects can ensue disrupting stability and enhancing the upward transport of heat and aerosol through turbulent motion (Barbaro et al., 2014; Huang et al., 2018). In continuation, previous studies found the role of aerosol on the suppression of ABL development through their relative heating and cooling in the upper atmosphere and surface, respectively (Liu et al., 2019; Petäjä et al., 2016; Wang et al., 2019b, 2020, 2018; Wilcox et al., 2016; Zhao et al., 2019; Zou et al., 2017)

Hence, understanding and characterising the regional transport of aerosols on the ABL structure and air quality are complex. There are studies signifying the role of aerosols on the boundary layer dynamics (Aruna et al., 2013; Huang et al., 2018; Ma et al., 2022; Miao and Liu, 2019; Raatikainen et al., 2014); however, most of them are based on the modelling framework, and observational evidence is scarce. This study aims to delineate, for the first time, the effects of transported aerosols from north India towards the southern part of the Indian peninsula on the boundary layer dynamics and hence the pollution dispersion using collocated high-resolution lidar, radiosondes, surface weather observations along with space-based observatories.

The Indo-Gangetic Plains (IGP), the densely populated and growing economy of the Indian subcontinent, experiences high aerosol loading both around the surface and in the vertical column during the winter season attributed to the wide range of anthropogenic activities ranging from biomass, fossil fuel burning and agricultural activities (Prasad et al., 2006; Ramanathan and Ramana, 2005; Tripathi et al., 2006). The prevalence of a high-pressure system over the central Indian landmass, especially during the winter seasons (December to March), generates a persistent northeasterly offshore flow (Krishnamurti et al., 1998). It provides a pathway for transporting aerosols from continental areas into the otherwise pristine ocean, covering thousands of kilometres in less than ten days (Krishnamurti et al., 1998; Rajeev et al., 2000). As such, pollutants from North India can get transported to the Bay of Bengal and then towards South India under the influence of prevalent strong convection and anticyclonic cyclonic circulation formation over the northwest of the Bay of Bengal (Prijith et al., 2016; Rajeevan and Srinivasan, 2000). Such transboundary transport of pollutants is evident in widespread pollution over the southern Indian peninsula (Ananthavel et al., 2021b; Kant et al., 2023; Mehta et al., 2023; Mhawish et al., 2022; Ratnam et al., 2018; Thomas et al., 2021). There is a campaign-based investigation held over the Indian Ocean, e.g., the Indian Ocean Experiment (INDOEX) (Ramanathan et al., 1995) to investigate the characteristics of transported aerosols towards the Indian Ocean and the Arabian Sea (Chester et al., 1991; Prodi et al., 1983; Savoie et al., 1989). The studies revealed that the transported aerosol predominantly consists of black carbon, organics, sulfate, nitrate, ammonia, sea salt, and mineral dust (Ramanathan et al., 2001). An increase in the aerosol loading in the free troposphere reduces the amount of incoming solar radiation reaching the surface, thus causing

https://doi.org/10.5194/egusphere-2024-3093
Preprint. Discussion started: 27 November 2024


dimming while warming the mid and upper troposphere and cooling the surface (Dipu et al., 2013; Sarangi et al., 2018). On the other hand, they significantly alter the atmosphere's underlying thermodynamics, leading to modifying the boundary layer structure. Hence, it is essential to characterise such transports, especially their occurrence characteristics and the nature of the aerosols present. However, observational evidence on such transboundary aerosol transports, their frequency of occurrences, their impact on the ABL development and the regional pollution maintenance have not been attempted yet; this study primarily focuses on unravelling such aspects.

Here, long-term satellite observations from Moderate Resolution Spectroradiometer (MODIS) and Cloud-Aerosol Lidar and Infrared Pathfinder Satellite Observatory (CALIPSO) are used to understand better and characterise the spatiotemporal variability in long-range regional transport of aerosols from North India to central-southern India during the winter season. Further, we have also used collocated observations of Micro Pulse Lidar, Radiosonde, surface weather and surface $PM_{2.5}$ measurements over Chennai to (i) investigate the widespread haziness over Chennai due to these regional aerosol transport episodes and (ii) quantify the associated changes in the surface meteorology, ABL height (ABL-H) and surface $PM_{2.5}$ distributions. Section 2 describes the datasets used, followed by the methodology for composite analysis of aerosols during the Regional Transport Episodes (RTE) days and clear days. Further, results and discussion are provided in section 4 and the conclusion in section 5.

## 2. Dataset and Methodology

### *Space-based observations*

MODIS on board the polar orbiting sun-synchronous satellites (Terra and Aqua) is utilised to estimate the aerosol optical depth (AOD) information at 550 nm. The MODIS measures radiance at 36 spectral bands in the visible to thermal IR spectral range of 0.41-14 µm (Kaufman et al., 1997). Within the spectral range, 7 bands are dedicated for aerosol measurement having a spatial resolution of 250m/500m. Owing to its large spatial swath (2330 km), MODIS is capable of observing the entire globe in a single day during two different times, i.e., at 01:30 AM/PM (Aqua) and 10:30 AM/PM (Terra) local time, which crosses the equator. We used the current version of Multiangle Implementation of Atmospheric Correction (MAIAC), which retrieves the AOD over land at 1 km resolution (Lyapustin et al., 2011b, 2011a), between December and March during 2015-2024 in this work.

In addition, the space-based lidar observation, Cloud-Aerosol Lidar with Orthogonal Polarization (CALIOP, (Winker et al., 2009; Young et al., 2013) onboard CALIPSO is utilised to understand the vertical variation of aerosol extinction profiles. The level 2, 5 km (horizontal averaged) aerosol profile (AProf) at 532 nm during December – March between 2015 and 2024, segregated during the RTE and clear days, are used. The CALIPSO crosses the equator ~01:30 AM/PM; however, only the night passes (~01:30 AM) are used for the present study owing to the better signal-to-noise ratio.

### *In situ observations*

The Micro Pulse Lidar (MPL), an elastic backscatter dual-polarization lidar of Droplet Measurement Techniques (DMT, USA), is located at the premise of SRM IST (45m above mean sea level). The instrument is set up at the Atmospheric Observation and Modelling Laboratory (AOML, 40m above the ground level), at a total height of

https://doi.org/10.5194/egusphere-2024-3093
Preprint. Discussion started: 27 November 2024


85m above mean sea level. The Normalised Relative Backscatter (NRB) is primarily utilised to retrieve total attenuated aerosol extinction and determine ABL-H. Details on site description and technical specifications about the MPL (Ali et al., 2022), retrieval of extinction coefficient and AOD (Ananthavel et al., 2021a, 2021b) and ABL-H estimation (Kakkanattu et al., 2023; Reddy et al., 2021a) are provided in references.

Upper air and surface weather information used in this study are obtained from India Meteorological Department (IMD) Chennai, from the sounding located at Meenambakkam (13.0N,80.06E, 16m above MSL), about 20.13 km northeast of SRM IST, Kattankulathur and Karaikal (10.9N,79.8E, 6.9m above MSL). The radiosonde data archived at 05:30 LT between December-January 2015 and 2024 are used to interpret the meteorological conditions during the aerosol transport periods and ABL-H determination. The gradient of potential temperature is utilised for the ABL-H determination (Mehta et al., 2017), where it is the altitude of the maximum potential temperature gradient at the lower troposphere.

Hourly $PM_{2.5}$ measurements are routinely made at the U.S. Embassy and Consulate, Chennai using a beta attenuation monitor (San Martini et al., 2015). The dataset within the study period is obtained from AirNow (http://www.airnow.gov). The $PM_{2.5}$ observations from the U.S. Embassy are validated and in good agreement with other observations (Jiang et al., 2015; Mukherjee and Toohey, 2016). The datasets are used to investigate the distribution of surface pollution during the haze transport from IGP to Chennai.

***MERRA2 Reanalysis Data Products***

The Modern Era Retrospective analysis for Research and Application, Version 2 (MERRA2) is employed to understand the spatial variation of Total Aerosol Extinction (TAE) and wind parameters (U, V, Speed). The MERRA2 reanalysis product provided by NASA's Global Modeling and Assimilation Office (GMAO) is available at 0.5° x 0.625° spatial resolution (Gelaro et al., 2017). MERRA2 simulates five aerosol species, including sulfate, black carbon, dust, organic carbon and sea salt, with Goddard Chemistry, Aerosol, Radiation and Transport (GOCART) model and their simulated properties are found to be robust (Randles et al., 2017).

**Methodology**

***Characterisation of RTE and Clear Sky days***

The RTE days are the days with significant aerosol transport from North India to the peninsular regions, inducing a widespread haziness over the areas. Such aerosol transports are identified from the spatial variation of AOD (MODIS), such that the AOD often exceeds 0.7 over the East Coast and nearby regions. Note that only days showing a visible transport from the IGP (See supplementary figure Fig. S1 for a reference) towards the south Indian peninsula are considered for the analysis. Conversely, there are days without any such transports; occurrences of such days often promote visibility and reduce the AOD significantly (less than 0.3) and termed them as 'clear' days. Note that days obscured with clouds, if any, are excluded from the entire segregation process of both RTE and clear days.

Further, CALIPSO swaths available during the RTE and clear days are segregated over the eastern coast within ±5° longitudes to study the spatial variation of extinction profiles pertinent to the corresponding events in addition to the MERRA2 (spatially across the Indian subcontinent) Total Aerosol Extinction (TAE) and wind products. Moreover, MPL (vertical profiles of extinction coefficient) and $PM_{2.5}$ measurements available during

https://doi.org/10.5194/egusphere-2024-3093
Preprint. Discussion started: 27 November 2024


RTE and clear days are segregated to infer the ABL-H variability and pollution concentration. Details of the sample available for the analysis are presented in Supplementary Table 1.

## 3. Results and Discussion

### 3.1 Occurrence of RTE and clear-sky days

The climatological mean spatial distribution of columnar AOD over the Indian subcontinent from RTE and clear days are compared in Fig. 1a and 1b. The significance of regional aerosol transport from north India to south during these months is evident as the composite mean AOD over the entire central and southeastern India during RTE days is 0.42±0.08 (Fig. 1a). The composite mean of AOD during clear days (Fig. 1b) is substantially lower (0.23±0.06) over the region; however, as expected, it was greater than 0.7 over the North India region. The RTE and clear days are observed to be 119 and 70 days, respectively, between 2015 and 2024. As discussed earlier, the RTE shows an enhancement of more than 0.7 over the eastern coast of India compared to the clear days.

The spatial distribution of aerosols during the RTE and clear days is further confirmed using the MERRA 2 reanalysis products. The average of the total aerosol extinction (TAE) obtained from MERRA 2 (equivalent to columnar AOD at 550 nm), superimposed with the wind vectors, for the same composite of RTE and clear-sky days are compared (Figure 1b-c). The analysis shows a similar pattern as observed from AOD distribution from satellite data; however, variation in the magnitudes is present. Notably, the TAE exceeds 60% on RTE days across the East Coast and nearby regions compared to clear days. During the winter and pre-monsoon season, the westerlies wind system is prominent over Northern India and IGP in the lower troposphere prevalent to the high-pressure system generation over central India (Krishnamurti et al., 1998). This flow manifests into a northerly wind as it enters the Bay of Bengal and eventually merges into the easterly circulation (prevalent around the tropics) as the wind enters back into the southern Peninsula, south of 20$^{o}$N. The fluctuations in this wind circulation and the intensity of the high-pressure system induce hazy or clear-sky days occurrences. We checked for any diurnal pattern in the TAE. However, such variations are negligible, pointing to the long-standing duration of such events. Hence, we further examined the endurance of RTE days. Normally, the RTE events prolong for days; persistence of such events for more than a day is observed to be ~53% of total observation, while 21% times it prolonged for more than 4 days

Duration of RTE episodes, in general, can vary from one day to 4-6 days. Fig. 1e provides an overview of such events' endurance between 2015 and 2024. Here, the number of consecutive RTE days occurrence (N) is estimated every year, and they are further segregated into distinct day duration bins; further, N is multiplied by the respective day duration to obtain the weighted count. The endurance of such events is colour-coded as black, magenta and red colours for single days, continuous for 2-4 days, and lasting for more than 4 days, respectively. Overall, endurance dominates the days exceedingly more than a day of RTE event. On average, the RTE which occurred over the south-eastern coast box for consecutive 2-4 days is the highest (as shown in Figure 1e), and such events show an increasing pattern. Notably, the year 2022 experienced a 12-day consecutive haziness between the 20$^{th}$ and 31$^{st}$ of March. Fig.1e also suggests an increasing trend in the overall occurrence of RTE days. Endurance of such hazy periods can result in significant consequences on the air quality and boundary layer dynamics. Note that, although a day between consecutive days is absent, e.g., the second day of three consecutive

https://doi.org/10.5194/egusphere-2024-3093
Preprint. Discussion started: 27 November 2024


days of an event, it is counted in this statistics to overcome the instrument limitation. It is worth noting that the easterly wind speed across the southern BoB is stronger during clear days than on RTE days. As such, the difference between the RTE and clear-day wind speed composites is that the wind speed during RTE days across the entire eastern half of the Indian subcontinent is weaker than the clear days (Fig 1f). The reduced wind speed is expected to promote the accumulation of aerosols and induce greater AOD over the south-eastern coast and the southern Indian peninsula, hence promoting the RTE.

The CALIOP observed mean vertical distribution of the aerosol extinction over the south-eastern coastal region (bounded box in the dotted line in Fig.1a and b) during the RTE days and clear-sky days is shown in Fig.2a and b, respectively. As expected, there is a distinct decreasing gradient in aerosol extinction values between surface and 2 km altitude as we move from IGP in the north to southern peninsular coastal India during both RTE and clear days. More interestingly, high values of aerosol extinction (> 0.15) are discernible up to 5 km during RTE days over the region south of 20$^{o}$N during RTE days, while the same is confined to altitudes less than 1.5 km during clear-sky days. Also, over region north of 20$^{o}$N, a relative increase in the extinction within ~2-4 km can be observed on RTE days relative to clear days. Several studies suggest the extension of aerosol layers more than 3 km. For instance, dust aerosols can reach up to 4-7 km during sandstorm episodes, as observed over the northwestern Tibet Plateau (Huang et al., 2007) and 3-5 km in urban Beijing (Guo et al., 2014). Using both CALIPSO and ground-based lidar measurements, (Qin et al., 2016) shows the transboundary transport of aerosols in China, having an aerosol layer depth of up to 3 km, during a haze event that occurred in the winter of 2015.

Temporal changes in the vertical characteristics of aerosol extinction, ABL and TAL during an RTE event followed by clear days, as observed by MPL, is provided in Fig.2b. Such that the vertical distribution of total attenuated aerosol extinction between 23-29 January 2018 which includes RTE episodes (24-27 January) and clear-sky conditions (23 and 28-29 January) as shown in Figure 2b. The figure also includes the vertical temperature profiles (T, radiosonde) and the ABL-H (MPL). The occurrence of the transported aerosol layer (TAL) can be seen above the ABL during the RTE periods and persisted for ~ 3-4 days. The top of the TAL (red dotted line) was identified as the prominent peak above the ABL, determined from the NRB gradient (Kakkanattu et al., 2023; Mehta et al., 2023). The TAL was observed initially at ~2.5 km at ~06:00 LT (or IST) on 24 January 2018, which gradually reduced to ~1.5 km and merged with the ABL at 09:00 LT on 28 January 2018. The temporal variation of background surface meteorology, including surface T, wind speed (WS), PM2.5 and the AOD, are provided in the Supplementary Figure Fig.S2. A significant increase in the columnar AOD between ~0.4 and 0.8 is observed during the hazy events. However, it maintains ~0.2-0.3 during the clear days. It is also worth noting that the AOD within the ABL (integrated extinction within surface and ABL-H) decreases from ~0.4 to less than 0.2 during the RTE period, suggesting a dominant presence of TAL above the ABL. Such aerosol accumulations are followed by strong upper atmospheric warming and surface cooling (Liu et al., 2019; Zhao et al., 2019). As discussed earlier, the atmosphere at the altitude, where the TAL presents, is observed to be warming. However, contrary to the earlier findings, the surface temperature is also observed to be warming. The effect of aerosols on the radiative forcing is mainly dominated by their microphysical characteristics, such as their absorption or scattering nature. Studies on such aspects are relied on in the future scope.

Interestingly, the ABL-H also decreased from ~1.4 km to ~0.3 km (~78% reduction) between 24 and 25 January 2018. The climatological ABL-H is observed to be 1.3±0.8 km and 1.8±0.8 km during the RTE and clear

https://doi.org/10.5194/egusphere-2024-3093
Preprint. Discussion started: 27 November 2024


days, respectively, exhibiting an overall reduction of ~38%, indicating the role of RTE events in altering the boundary layer dynamics. The suppression of the ABL followed by accumulation of absorptive aerosol in the upper ABL has been investigated earlier, especially through numerical simulations (Ding et al., 2013, 2016; Zhao et al., 2019); however, observational evidence is scarce. (Barbaro et al., 2014) suggests that a drop in the ABL from 1.4 km to 0.9 km (~35% reduction), through sensitivity experiments. Similarly, (Wang et al., 2015) suggest that the stable stratification of the atmosphere above the ABL through the significant warming by absorbing aerosols contributed to a decrease of ABL-H by 33%. Observational studies over China suggest that the occurrence of elevated aerosol layers has induced suppression of ABL-H from 1.27 km to 0.78 km (~38% reduction) hence lifting the surface pollution level to 118% (Wang et al., 2018). (Zhang et al., 2021b) reports a reduction in the ABL-H from 1.09 km to 0.48 (~60% reduction) during intense haze episodes over China. Unfortunately, observational evidence of such aspects is not attempted over peninsular India, especially when transport events occur. The temperature profiles (Fig.2c) show a strong inversion at the altitude of ABL and the top of the TAL during the hazy days, attributed to the aerosol heating. This contention further suggests that the presence of strong temperature inversion over the ABL, especially during the dry season, can be accounted for the presence of TAL followed by widespread haziness, increased temperature and pollution.

The study further extends to the diurnal changes in the aerosol extinction. Fig.2d shows the diurnal variation of difference in total aerosol extinction during the available RTE (10 days) and clear (6 days) day cases within 2018 and 2023 obtained from MPL. Notably, a strong enhancement in the extinction coefficient during RTE days is discernible, especially above the ABL with a thickness of ~1.5-2 km; however, an overall reduction is observed within the ABL except during the forenoon hours. The accumulation of such aerosols can strongly impact the evolution of ABL. Fig.S3 shows the scatter plot between the ABL-H and AOD observed above the ABL ($AOD_{aloft}$, integrated extinction above ABL-H), showing a strong inverse relation with a statistically significant correlation of -0.42. It points out that the observed reduction in the ABL-H prevalent to the RTE is linked to the optical depth of the aerosol aloft. Additionally, the enhancement in the aerosol extinction in the atmosphere (both the scattering and absorption of sunlight) can significantly reduce the short-wave radiation of incoming solar radiation, hence reducing the surface heat flux and development of ABL, resulting in the inhibition of ABL-H (Ding et al., 2013; Li et al., 2017; Petäjä et al., 2016; Quan et al., 2013). On the other hand, absorbing aerosols can heat the atmosphere, leading to temperature inversion (Xu et al., 2019). It is also worth noting that the surface extinction during the RTE days increased during the forenoon hours. Such enhancement can significantly impact the $PM_{2.5}$ dispersion during those periods. Inhibition of ABL development by the strong absorbing aerosols in the upper ABL can trigger high concentrations of pollution at the surface (Ding et al., 2016; Petäjä et al., 2016; Zou et al., 2017) and such aspects are discussed in Sec. 3.3.

### 3.2 Meteorological conditions during RTE and clear days

To understand the effect of the transported aerosols and their vertical extent on the background metrological conditions, we also analysed the vertical profiles of the wind speed (WS), relative humidity (RH) and temperature (T) obtained from radiosonde observations over the two coastal stations; Chennai (13.0°N, 80.0°E) and Karaikal (10.92°N, 79.83°E), located in the east coast of the Indian peninsula where Karaikal is

https://doi.org/10.5194/egusphere-2024-3093
Preprint. Discussion started: 27 November 2024


departed by ~240 km from Chennai. The average profiles with standard error obtained for the RTE (red) and clear (blue) categories are shown separately for Chennai and Karaikal, the first and second raw panels. The difference between the RTE and clear days (RTE-Clear) is shown on the top axis as dashed lines. Although the wind direction is north easterlies up to 3 km in both stations, the WS varies during the RTE and clear days. The WS up to 3 km is almost similar to that of Chennai and Karaikal during the RTE days except at the surface. However, it exceeded by ~2 m/s during clear days over both stations. The WS is observed to get stronger above ~1.5 km during the RTE days. Such an enhancement in the WS can favour the transport from IGP and accumulate over the boundary layer. However, the overall WS during RTE days remains calmer than on clear days. The effect of the accumulated aerosol on the boundary layer processes majorly depends on the aerosol characteristics. For instance, the absorption aerosol concentration above the ABL heats the thermal inversion layer and strongly suppresses the ABL development (dome effect) (Ma et al., 2020). The shallow ABL further promote severe hazy episodes (Quan et al., 2014; Ye et al., 2016). On the other hand, the radiative impact of the aerosols and their feedback on the haze can further intensify the pollution (Ding et al., 2016; Yang et al., 2016).

A rapid decline in the RH from ~80% to 50% is observed during RTE days between the surface and 1.5 km (Fig.3b and e). However, it gradually decreases from ~80% to 40% during the clear days. In general, the persistence of such RH above the boundary layer is expected to enhance the hygroscopic growth of the transported aerosol layer and thus increase their endurance period (Zhao et al., 2017). However, compared to clear days, it observes a rapid decline in the RH up to ~20% during the RTE days till ~ 1 km. This contention further points to the absence of the hygroscopic growth of aerosol above the ABL; rather, the pollutants are mostly transported, favoured by the prevalent wind system. Notably, a strong increase in the temperature is observed within ~1.5 km is during RTE days (Fig.3c). Although Karaikal experienced an enhancement of ~1.2 K, Chennai peaks to ~2.5 K. Such increment in the T suggests the radiative effects of transported aerosol on the boundary layer. This phenomenon also suggests that aerosol-induced warming at the lower troposphere not only increases the temperature at the altitude where aerosol lies but also modifies the overall temperature profiles of the lower atmosphere. Observational study by (Huang et al., 2018) over Northern China region shows a significant heating in the upper ABL, where the aerosol accumulation is more, with a maximum temperature change of ~0.7°C on average. Recent studies suggest that the occurrence of the aerosol layer in lower troposphere warming while inducing a strong inhibition layer, and it may further promote extreme precipitation events (Dagan and Eytan, 2024).

Considering Chennai and Karaikal stations, although the WS and RH variation during the RTE and clear days are similar, the observed change in the temperature varies significantly regardless of the limited distance between the two stations (~2° meridionally). It suggests the spatial inhomogeneity in the TAL distribution. A reduction in the AOD distribution by ~20-22% (from~ 0.9 to 0.7) (Fig.1a) between Chennai and Karaikal decreased ~1K or 35-40% (from ~2.5 to 1.5) of regional temperature. Additionally, the surface is observed to be less warm over Karaikal compared to Chennai during the RTE days.

### 3.3 Effect of transported aerosols on the boundary layer and air quality

As mentioned earlier, the occurrence of RTE induces a strong warming around the top of ABL. Such warming is expected to change the vertical temperature stratification and thus impede the development of ABL,

https://doi.org/10.5194/egusphere-2024-3093
Preprint. Discussion started: 27 November 2024


commonly termed as "dome effect" of aerosols (Ding et al., 2016). Figure 4a examines the difference between the temperature between 1.5 km and surface (ΔT) during the RTE and clear cases. Although clear cases distribution peak maximizes around -8°C, the RTE skews towards -4°C, showing the relative role of transported aerosol on the temperature stratification and inducing the "dome effect". The relative suppression of ABL development under the influence of TAL is shown in Figure 4b.

Figure 4b shows the probability distribution of ABL-H estimated from the radiosonde profiles over Chennai during both the RTE and clear days. Interestingly, the PDF during RTE days peaks around ~0.5 km while it is 2-2.5 km during the clear days. Skewness of ABL-H distribution towards the lower altitudes, especially during the RTE days, suggests the relative role of TAL on the suppression of ABL. Such suppression in the ABL-H was dominant during the afternoon hours, as observed from the MPL (see Fig.2b). The development of ABL during daytime is mainly dominated by convective processes (Garratt, 1994; Stull, 1988); however, the formation of TAL suppresses such development, hence reducing the ABL-H. On the other hand, the complex radiative interaction between the incoming solar radiation with the TAL, especially the surface dimming and inducement of the "dome effect", can also affect the development of ABL (Guo et al., 2017; Petäjä et al., 2016). The solar dimming due to the presence of TAL can block the solar radiation reaching the surface, resulting in the overall dimming in the ground surface, weakening the surface flux, perturbing the convective process and suppressing the ABL development. Enhancement in the suppression of ABL-H distribution during the afternoon hours can also be attributed to the thermal internal boundary layer formation, where the transport of pollutants towards the land from BoB under the influence of sea breeze (Reddy et al., 2021b). However, this contention requires further investigation with large samples. As mentioned earlier, the suppression of ABL-H in the presence of TAL could substantially enhance near-surface haze pollution (Petäjä et al., 2016; Sun et al., 2024; Zou et al., 2017).

The association of ABL-H and $PM_{2.5}$ is delineated using collocated observations of MPL and $PM_{2.5}$ measurements over Chennai. The RTE days where MPL is operational are only used for this analysis. Fig.4d shows the scatter of normalised anomalies between $PM_{2.5}$ and ABL-H. The normalised anomalies are obtained by subtracting the parameters from the climatological average (during the winter season) and further divided with the same ($X\ Anom. = \frac{X - X_{Climatology}}{X_{Climatology}}$, where X = $PM_{2.5}$, ABL-H). Note that, average ABL-H during the winter season is estimated with the NRB during 2018 and 2023 alone. However, it matches with the climatological ABL-H estimated by (Reddy et al., 2021a) over Chennai. Interestingly, the normalised anomalies between $PM_{2.5}$ and ABL-H are negatively related, with a statistically significant (>95% confidence) correlation of -0.38. It portrays that, overall, a 50% reduction in the ABL-H contributed to ~100-150% increase in the surface $PM_{2.5}$ concentrations. Observational studies by (Su et al., 2020) show a nearly similar relationship during COVID-19 in China; however, with a different correlation value over Beijing and Northern China, attributed to the inhomogeneity in the spatial distribution of pollution. It is to be noted that, the wind speed and direction are the major influencing factors affecting the spatial distribution of aerosols. Hence, we further analysed the contribution of WS and WD explicitly. The observed negative association becomes stronger when the WS exceeds more than 4 m/s (-0.46, N=40) and also when the WD from the northeast direction (-0.5, N=56). Such cases show the $PM_{2.5}$ aggravation to ~150-200% when the ABL-H suppressed by 50% (Fig.4d). It suggests that RTE favoured by the enhanced WS, directed from north India, influences the formation and maintenance of TAL over the southern

https://doi.org/10.5194/egusphere-2024-3093
Preprint. Discussion started: 27 November 2024


Indian regions, and it further suppresses the local boundary layer while increasing the surface pollution concentration.

In general, an increased ABL height, as usually occurs during clear days, can result in acceleration of surface wind speed and enhanced vertical movement (Xiang et al., 2019), promoting reduced surface pollution. On the other hand, the occurrence of residual layer (RL) or stable boundary layer (SBL) complicates the pollution dynamics at the surface (Yu et al., 2020). The observed anomalies in the surface pollution in the cases of clear days can be attributed to the re-entrainment of pollutants in the RL into the mixed layer, leading to rapid change in the surface pollution concentration (Shi et al., 2020; Yu et al., 2020). In addition, the presence of SBL, which hinders the exchange of pollutants and energy between the surface and free atmosphere, potentially leads to higher concentrations of pollutants in the atmosphere if they are not cleared otherwise (Shi et al., 2020), similar to the RTE conditions.

Finally, the overall diurnal changes in $PM_{2.5}$ during the RTE and clear day composites are portrayed in Fig.4d. As expected, the RTE days experience ~30-35% enhancement in $PM_{2.5}$ than clear days. The surface $PM_{2.5}$ increases during the early morning hours and maximizes at 08:00 LT. Although the clear-day composite shows a gradual decrease from 50 $\mu g/m^3$ to 30 $\mu g/m^3$ between 08:00 and 15:00 LT, it rapidly decreases from 60 $\mu g/m^3$ to 32 $\mu g/m^3$ during RTE days. As depicted in Fig.2d, the enhancement in the aerosol extinction coefficient is minimal during the afternoon hours during the RTE days. The observed variation in surface pollution is also linked with the ABL-H. An increase in the ABL-H makes a pathway for the dispersion of air pollutants, hence reducing surface pollution levels. In contrast, a suppressed ABL-H significantly affect the vertical dispersion, leading to higher concentrations of pollutants near the surface (Wang et al., 2019a).

## 4 Summary and Conclusion

This paper presents the first observational evidence of the effect of transboundary transported aerosols on the boundary layer dynamics and pollution dispersion over the east coast regions of peninsular India. The aerosol transport from IGP towards south India is segregated from the spatial distribution of AOD using MODIS. Such transboundary transports (referred to as RTE), mainly influenced by the anticyclonic circulation formation over the northern BoB and prevalent north easterlies, contribute widespread haziness spatially and vertically over the west coast of BoB and nearby regions.

The occurrence of RTE days generally prolongs for more than a day. The largest lapsed RTE were observed during March 2022, which continued for 12 consecutive days. The widespread haziness over the northeastern region of the Indian subcontinent induced by the occurrence of TAL, especially during the winter season, is mainly favoured by the relative reduction of wind speed during the season near the surface. The reduced windspeed declines the dispersion of pollutants over a large area in the southern Indian peninsula hence reducing any diurnal variability in the aerosol distribution. On the other hand, although the overall WS declines during RTE days compared to clear days, it shows some enhancement above ~1.5 km, promoting the formation and growth of TAL aloft the ABL.

The TAL has a ~1-2 km thickness and occurs just above the ABL. A strong temperature inversion between the top of the TAL and free troposphere is observed during the RTE periods, followed by a strong warming up to ~1-1.5°C where the TAL is present. Overall, the RTE and occurrence of TAL have suppressed the ABL-H by

https://doi.org/10.5194/egusphere-2024-3093
Preprint. Discussion started: 27 November 2024


~38%; however, for a typical RTE episode, temporal variation in the aerosol extinction characteristic suggests a suppression of up to ~78 %. The occurrence and maintenance of TAL during the RTE are favoured by the strong wind flow from north India, which majorly contributes to the reduction of the ABL-H and aggravation of surface pollution. The aerosol "dome effect", as a result of the vertical temperature stratification due to the presence of TAL, has induced the suppression of the ABL-H and increased the surface $PM_{2.5}$ by ~30-35% compared to the clear days. This study elucidates the first qualitative investigation of the transboundary transport of aerosols over the Indian peninsula and is a reference for emission policies over the eastern coasts, especially over Chennai and the surrounding area. The analysis of the TAL is carried out by removing the cases of shallow clouds occurring frequently during the study period, which we would like to pursue in a future study.

**Data Availability**

MODIS and MERRA2 data can be obtained from NASA Goddard Earth Sciences Data and Information Services Center (GES DISC). CALIPSO data used in this study can be obtained directly from the website https://eosweb.larc.nasa.gov/project/calipso/calipso_table. Radiosonde and surface data can be obtained from the https://weather.uwyo.edu/upperair/sounding.html. The MPL data used in this study are not publicly available; however, the data can be provided to the corresponding author upon request.

**Author contributions**.

SA was responsible for carrying out the investigation, writing, reviewing, data curation, and preparing the original draft of the paper. CS is responsible for conceptualizing and supervising the study, carrying out the investigation, writing, reviewing, and editing the paper. SKM is responsible for reviewing and editing the paper

**Competing interests.**

The contact author has declared that neither they nor their co-authors have any competing interests

**Acknowledgements**

SA thanks the Asia-Pacific Network for Global Change Research (APN) research grant (CRRP2022-08MY-Sarangi) for supporting this work

https://doi.org/10.5194/egusphere-2024-3093
Preprint. Discussion started: 27 November 2024


408 **Figures.**

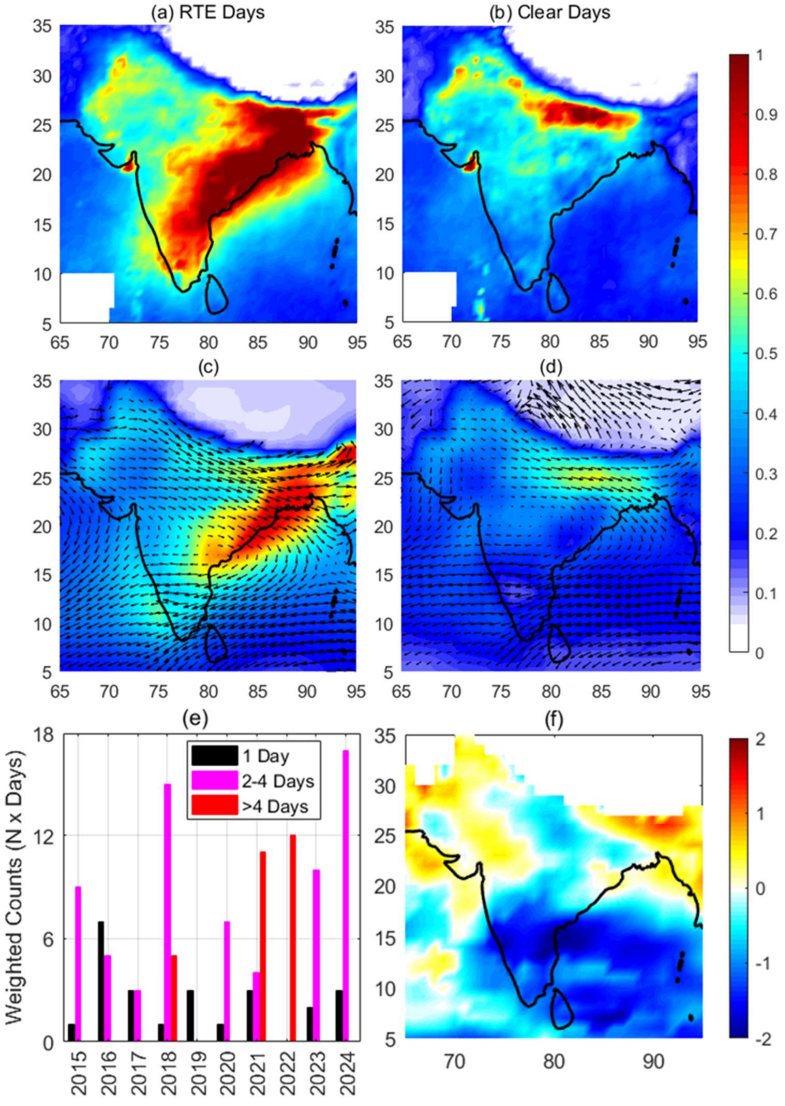


409

410 **Figure 1 Composite of the spatial distribution of AOD obtained from MODIS during (a) RTE and (b) clear**
411 **days between December and March during 2015-2024 and total aerosol extinction (TAE) from MERRA2**
412 **reanalysis dataset observed for the composite of (c) RTE and (d) clear days. Panel (e) shows the statistics of**
413 **occurrence frequency of RTE day periods segregated for 1 day (black), 2-4 days (magenta) and more than**
414 **4 days (red). (f) Difference in the wind speed between RTE and clear days at 850 hPa.**

415

https://doi.org/10.5194/egusphere-2024-3093
Preprint. Discussion started: 27 November 2024


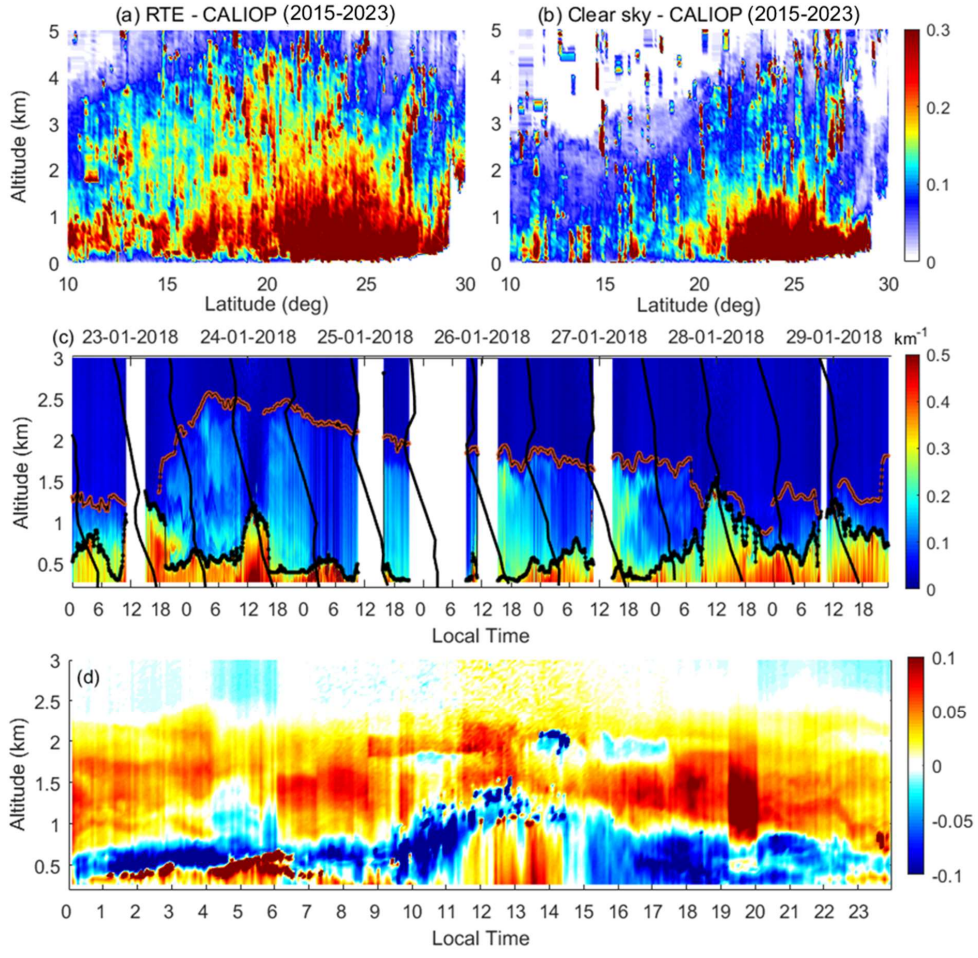


**Figure 2. The vertical distribution of the aerosol extinction coefficient from CALIOP during the (a) RTE and (b) clear days within ±4° longitude over the eastern coast of India between December and March 2015-2023. (c) Time-Altitude cross-section of the total attenuated extinction coefficient obtained from Micro Pulse Lidar (MPL) observation over Chennai (SRM IST) between 23 and 29 January 2018. The black line corresponds to the temperature profiles from radiosonde over IMD, Chennai. The black dotted line corresponds to the derived ABL-H, and the red dotted lines are the top of the transported aerosol layer (d) Temporal changes in the mean difference between the extinction coefficients during the available RTE and clear day composites (RTE – Clear) from MPL observations.**

https://doi.org/10.5194/egusphere-2024-3093
Preprint. Discussion started: 27 November 2024


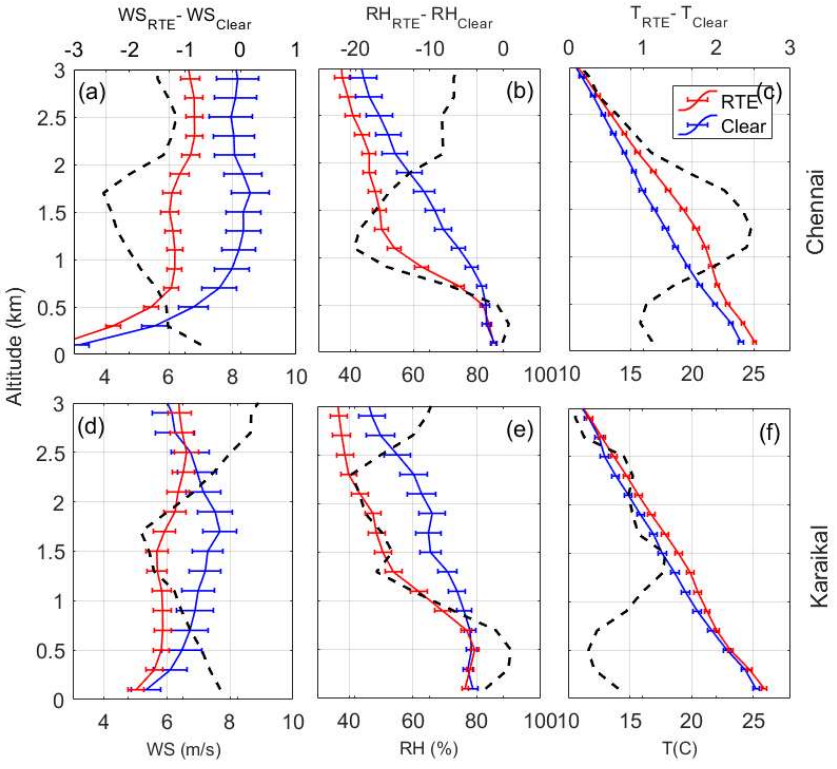


**Figure 3 Vertical variation of Wind Speed (WS), Relative Humidity (RH) and Temperature (T) over Chennai (a-c) and Karaikal (d-f) during RTE (red) and (b) clear days (blue). The difference in the RTE and clear days (RTE-Clear) are shown in dashed line (axes in top). The horizontal bars correspond to the standard errors.**

https://doi.org/10.5194/egusphere-2024-3093
Preprint. Discussion started: 27 November 2024


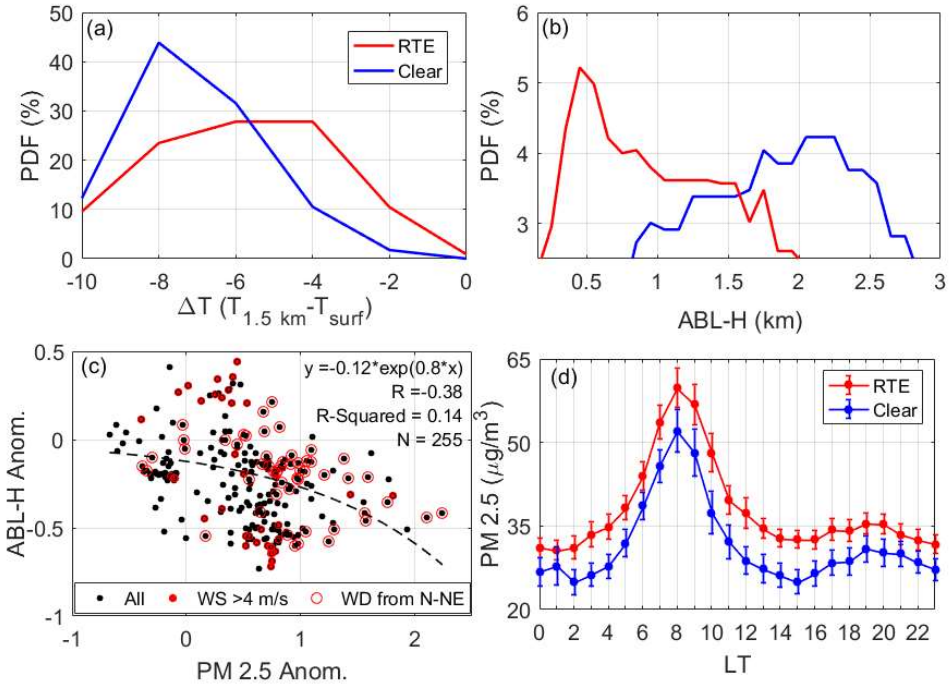


**Figure 4. Probability distribution (%) of (a) difference in temperature between 1.5 km and surface (ΔT; bin size=2K) and the (b) ABL-H obtained during climatological RTE (red) and clear (blue) cases (bin size=0.2km). (c) Scatter plot showing the normalized anomaly of PM 2.5 and ABL-H (obtained from MPL) during the RTE days as observed by MPL. The red scatters show the cases when wind speed (WS) is exceeds 4 m/s and red circles for the cases where wind directed from north to north east. The correlation coefficient, exponential fit (dashed line) equation, $R^2$ and number of samples also provided. (d) Diurnal variation of $PM_{2.5}$ over Chennai (US Consulate, Chennai) during RTE and clear days.**

https://doi.org/10.5194/egusphere-2024-3093
Preprint. Discussion started: 27 November 2024


**References:**

Ali, S., Mehta, S. K., Ananthavel, A. and Reddy, T. V. R.: Temporal and vertical distributions of the occurrence of cirrus clouds over a coastal station in the Indian monsoon region, Atmos. Chem. Phys., 22(12), 8321–8342, doi:10.5194/acp-22-8321-2022, 2022.

Ananthavel, A., Mehta, S. K., Ali, S., Reddy, T. V. R., Annamalai, V. and Rao, D. N.: Micro Pulse Lidar measurements in coincidence with CALIPSO overpasses: Comparison of tropospheric aerosols over Kattankulathur (12.82oN, 80.04oE), Atmos. Pollut. Res., 12(6), 101082, doi:10.1016/j.apr.2021.101082, 2021a.

Ananthavel, A., Mehta, S. K., Reddy, T. V. R., Ali, S. and Rao, D. N.: Vertical distributions and columnar properties of the aerosols during different seasons over Kattankulathur (12.82oN, 80.04oE): A semi-urban tropical coastal station, Atmos. Environ., 256, 118457, doi:10.1016/j.atmosenv.2021.118457, 2021b.

Aruna, K., Kumar, T. V. L., Rao, D. N., Murthy, B. V. K., Babu, S. S. and Moorthy, K. K.: Black carbon aerosols in a tropical semi-urban coastal environment: Effects of boundary layer dynamics and long range transport, J. Atmos. Solar-Terrestrial Phys., 104, 116–125, doi:10.1016/j.jastp.2013.08.020, 2013.

Barbaro, E., de Arellano, J. V., Ouwersloot, H. G., Schröter, J. S., Donovan, D. P. and Krol, M. C.: Aerosols in the convective boundary layer: Shortwave radiation effects on the coupled land-atmosphere system, J. Geophys. Res. Atmos., 119(10), 5845–5863, doi:10.1002/2013JD021237, 2014.

Chester, R., Berry, A. S. and Murphy, K. J. T.: The distributions of particulate atmospheric trace metals and mineral aerosols over the Indian Ocean, Mar. Chem., 34(3–4), 261–290, doi:10.1016/0304-4203(91)90007-J, 1991.

Comstock, J. M. and Sassen, K.: Retrieval of cirrus cloud radiative and backscattering properties using combined lidar and infrared radiometer (LIRAD) measurements, J. Atmos. Ocean. Technol., 18(10), 1658–1673, doi:10.1175/1520-0426(2001)018<1658:ROCCRA>2.0.CO;2, 2001.

Dagan, G. and Eytan, E.: The Potential of Absorbing Aerosols to Enhance Extreme Precipitation, Geophys. Res. Lett., 51(10), doi:10.1029/2024GL108385, 2024.

Ding, A. J., Fu, C. B., Yang, X. Q., Sun, J. N., Petäjä, T., Kerminen, V.-M., Wang, T., Xie, Y., Herrmann, E., Zheng, L. F., Nie, W., Liu, Q., Wei, X. L. and Kulmala, M.: Intense atmospheric pollution modifies weather: a case of mixed biomass burning with fossil fuel combustion pollution in eastern China, Atmos. Chem. Phys., 13(20), 10545–10554, doi:10.5194/acp-13-10545-2013, 2013.

Ding, A. J., Huang, X., Nie, W., Sun, J. N., Kerminen, V. -M., Petäjä, T., Su, H., Cheng, Y. F., Yang, X. -Q., Wang, M. H., Chi, X. G., Wang, J. P., Virkkula, A., Guo, W. D., Yuan, J., Wang, S. Y., Zhang, R. J., Wu, Y. F., Song, Y., Zhu, T., Zilitinkevich, S., Kulmala, M. and Fu, C. B.: Enhanced haze pollution by black carbon in megacities in China, Geophys. Res. Lett., 43(6), 2873–2879, doi:10.1002/2016GL067745, 2016.

Dipu, S., Prabha, T. V., Pandithurai, G., Dudhia, J., Pfister, G., Rajesh, K. and Goswami, B. N.: Impact of elevated aerosol layer on the cloud macrophysical properties prior to monsoon onset, Atmos. Environ., 70, 454–467, doi:10.1016/j.atmosenv.2012.12.036, 2013.

Garratt, J.: Review: the atmospheric boundary layer, Earth-Science Rev., 37(1–2), 89–134, doi:10.1016/0012-8252(94)90026-4, 1994.

Gelaro, R., McCarty, W., Suárez, M. J., Todling, R., Molod, A., Takacs, L., Randles, C. A., Darmenov, A., Bosilovich, M. G., Reichle, R., Wargan, K., Coy, L., Cullather, R., Draper, C., Akella, S., Buchard, V., Conaty, A., da Silva, A. M., Gu, W., Kim, G.-K., Koster, R., Lucchesi, R., Merkova, D., Nielsen, J. E., Partyka, G., Pawson, S., Putman, W., Rienecker, M., Schubert, S. D., Sienkiewicz, M. and Zhao, B.: The Modern-Era Retrospective Analysis for Research and Applications, Version 2 (MERRA-2), J. Clim., 30(14), 5419–5454, doi:10.1175/JCLI-D-16-0758.1, 2017.

Guo, J., Xia, F., Zhang, Y., Liu, H., Li, J., Lou, M., He, J., Yan, Y., Wang, F., Min, M. and Zhai, P.: Impact of diurnal variability and meteorological factors on the PM2.5 - AOD relationship: Implications for PM2.5 remote sensing, Environ. Pollut., 221, 94–104, doi:10.1016/j.envpol.2016.11.043, 2017.

Guo, S., Hu, M., Zamora, M. L., Peng, J., Shang, D., Zheng, J., Du, Z., Wu, Z., Shao, M., Zeng, L., Molina, M. J. and Zhang, R.: Elucidating severe urban haze formation in China, Proc. Natl. Acad. Sci., 111(49), 17373–17378, doi:10.1073/pnas.1419604111, 2014.

https://doi.org/10.5194/egusphere-2024-3093
Preprint. Discussion started: 27 November 2024


Haywood, J. and Boucher, O.: Estimates of the direct and indirect radiative forcing due to tropospheric aerosols: A review, Rev. Geophys., 38(4), 513–543, doi:10.1029/1999RG000078, 2000.

Huang, J., Minnis, P., Yi, Y., Tang, Q., Wang, X., Hu, Y., Liu, Z., Ayers, K., Trepte, C. and Winker, D.: Summer dust aerosols detected from CALIPSO over the Tibetan Plateau, Geophys. Res. Lett., 34(18), doi:10.1029/2007GL029938, 2007.

Huang, X., Wang, Z. and Ding, A.: Impact of Aerosol-PBL Interaction on Haze Pollution: Multiyear Observational Evidences in North China, Geophys. Res. Lett., 45(16), 8596–8603, doi:10.1029/2018GL079239, 2018.

Jiang, J., Zhou, W., Cheng, Z., Wang, S., He, K. and Hao, J.: Particulate Matter Distributions in China during a Winter Period with Frequent Pollution Episodes (January 2013), Aerosol Air Qual. Res., 15(2), 494–503, doi:10.4209/aaqr.2014.04.0070, 2015.

Kakkanattu, S. P., Mehta, S. K., Purushotham, P., Betsy, K. B., Seetha, C. J. and Musaid, P. P.: Continuous monitoring of the atmospheric boundary layer (ABL) height from micro pulse lidar over a tropical coastal station, Kattankulathur (12.82° N, 80.04° E), Meteorol. Atmos. Phys., 135(1), 2, doi:10.1007/s00703-022-00938-x, 2023.

Kant, S., Sarangi, C. and Wilcox, E. M.: Aerosol processes perturb cloud trends over Bay of Bengal: observational evidence, npj Clim. Atmos. Sci., 6(1), 132, doi:10.1038/s41612-023-00443-x, 2023.

Kaufman, Y. J., Wald, A. E., Remer, L. A., Bo-Cai Gao, Rong-Rong Li and Flynn, L.: The MODIS 2.1-μm channel-correlation with visible reflectance for use in remote sensing of aerosol, IEEE Trans. Geosci. Remote Sens., 35(5), 1286–1298, doi:10.1109/36.628795, 1997.

Krishnamurti, T. N., Jha, B., Prospero, J., Jayaraman, A. and Ramanathan, V.: Aerosol and pollutant transport and their impact on radiative forcing over the tropical Indian Ocean during the January–February 1996 pre-INDOEX cruise, Tellus B Chem. Phys. Meteorol., 50(5), 521, doi:10.3402/tellusb.v50i5.16235, 1998.

Li, Z., Guo, J., Ding, A., Liao, H., Liu, J., Sun, Y., Wang, T., Xue, H., Zhang, H. and Zhu, B.: Aerosol and boundary-layer interactions and impact on air quality, Natl. Sci. Rev., 4(6), 810–833, doi:10.1093/nsr/nwx117, 2017.

Liu, G., Xin, J., Wang, X., Si, R., Ma, Y., Wen, T., Zhao, L., Zhao, D., Wang, Y. and Gao, W.: Impact of the coal banning zone on visibility in the Beijing-Tianjin-Hebei region, Sci. Total Environ., 692, 402–410, doi:10.1016/j.scitotenv.2019.07.006, 2019.

Lohmann, U. and Feichter, J.: Global indirect aerosol effects: a review, Atmos. Chem. Phys., 5(3), 715–737, doi:10.5194/acp-5-715-2005, 2005.

Lyapustin, A., Wang, Y., Laszlo, I., Kahn, R., Korkin, S., Remer, L., Levy, R. and Reid, J. S.: Multiangle implementation of atmospheric correction (MAIAC): 2. Aerosol algorithm, J. Geophys. Res., 116(D3), D03211, doi:10.1029/2010JD014986, 2011a.

Lyapustin, A., Smirnov, A., Holben, B., Chin, M., Streets, D. G., Lu, Z., Kahn, R., Slutsker, I., Laszlo, I., Kondragunta, S., Tanré, D., Dubovik, O., Goloub, P., Chen, H.-B., Sinyuk, A., Wang, Y. and Korkin, S.: Reduction of aerosol absorption in Beijing since 2007 from MODIS and AERONET, Geophys. Res. Lett., 38(10), n/a-n/a, doi:10.1029/2011GL047306, 2011b.

Ma, Y., Ye, J., Xin, J., Zhang, W., Vilà-Guerau de Arellano, J., Wang, S., Zhao, D., Dai, L., Ma, Y., Wu, X., Xia, X., Tang, G., Wang, Y., Shen, P., Lei, Y. and Martin, S. T.: The Stove, Dome, and Umbrella Effects of Atmospheric Aerosol on the Development of the Planetary Boundary Layer in Hazy Regions, Geophys. Res. Lett., 47(13), doi:10.1029/2020GL087373, 2020.

Ma, Y., Xin, J., Wang, Z., Tian, Y., Wu, L., Tang, G., Zhang, W., de Arellano, J. V.-G., Zhao, D., Jia, D., Ren, Y., Gao, Z., Shen, P., Ye, J. and Martin, S. T.: How do aerosols above the residual layer affect the planetary boundary layer height?, Sci. Total Environ., 814, 151953, doi:10.1016/j.scitotenv.2021.151953, 2022.

Mehta, S. K., Ojha, D., Mehta, S., Anand, D., Rao, D. N., Annamalai, V., Ananthavel, A. and Ali, S.: Thermodynamic structure of the convective boundary layer ( CBL ) over the Indian monsoon region during CAIPEEX campaigns, , (iv), 1361–1379, 2017.

Mehta, S. K., Ananthavel, A., Velu, V., Prabhakaran, T., Pandithurai, G. and Rao, D. N.: Characteristics of elevated aerosol layer over the Indian east coast, Kattankulathur (12.82oN, 80.04°E): A northeast monsoon region,

https://doi.org/10.5194/egusphere-2024-3093
Preprint. Discussion started: 27 November 2024


Sci. Total Environ., 886, 163917, doi:10.1016/j.scitotenv.2023.163917, 2023.

Mhawish, A., Sarangi, C., Babu, P., Kumar, M., Bilal, M. and Qiu, Z.: Observational evidence of elevated smoke layers during crop residue burning season over Delhi: Potential implications on associated heterogeneous PM2.5 enhancements, Remote Sens. Environ., 280, 113167, doi:10.1016/j.rse.2022.113167, 2022.

Miao, Y. and Liu, S.: Linkages between aerosol pollution and planetary boundary layer structure in China, Sci. Total Environ., 650, 288–296, doi:10.1016/j.scitotenv.2018.09.032, 2019.

Mukherjee, A. and Toohey, D. W.: A study of aerosol properties based on observations of particulate matter from the U.S. Embassy in Beijing, China, Earth's Futur., 4(8), 381–395, doi:10.1002/2016EF000367, 2016.

Petäjä, T., Järvi, L., Kerminen, V.-M., Ding, A. J., Sun, J. N., Nie, W., Kujansuu, J., Virkkula, A., Yang, X., Fu, C. B., Zilitinkevich, S. and Kulmala, M.: Enhanced air pollution via aerosol-boundary layer feedback in China, Sci. Rep., 6(1), 18998, doi:10.1038/srep18998, 2016.

Prasad, A. K., Singh, R. P. and Kafatos, M.: Influence of coal based thermal power plants on aerosol optical properties in the Indo-Gangetic basin, Geophys. Res. Lett., 33(5), doi:10.1029/2005GL023801, 2006.

Prijith, S. S., Rao, P. V. N. and Mohan, M.: Genesis of elevated aerosol loading over the Indian region, edited by T. N. Krishnamurti and M. N. Rajeevan, p. 988208., 2016.

Prodi, F., Santachiara, G. and Oliosi, F.: Characterization of aerosols in marine environments (Mediterranean, Red Sea, and Indian Ocean), J. Geophys. Res. Ocean., 88(C15), 10957–10968, doi:10.1029/JC088iC15p10957, 1983.

Qin, K., Wu, L., Wong, M. S., Letu, H., Hu, M., Lang, H., Sheng, S., Teng, J., Xiao, X. and Yuan, L.: Trans-boundary aerosol transport during a winter haze episode in China revealed by ground-based Lidar and CALIPSO satellite, Atmos. Environ., 141, 20–29, doi:10.1016/j.atmosenv.2016.06.042, 2016.

Quan, J., Gao, Y., Zhang, Q., Tie, X., Cao, J., Han, S., Meng, J., Chen, P. and Zhao, D.: Evolution of planetary boundary layer under different weather conditions, and its impact on aerosol concentrations, Particuology, 11(1), 34–40, doi:10.1016/j.partic.2012.04.005, 2013.

Quan, J., Tie, X., Zhang, Q., Liu, Q., Li, X., Gao, Y. and Zhao, D.: Characteristics of heavy aerosol pollution during the 2012–2013 winter in Beijing, China, Atmos. Environ., 88, 83–89, doi:10.1016/j.atmosenv.2014.01.058, 2014.

Raatikainen, T., Hyvärinen, A.-P., Hatakka, J., Panwar, T. S., Hooda, R. K., Sharma, V. P. and Lihavainen, H.: The effect of boundary layer dynamics on aerosol properties at the Indo-Gangetic plains and at the foothills of the Himalayas, Atmos. Environ., 89, 548–555, doi:10.1016/j.atmosenv.2014.02.058, 2014.

Rajeev, K., Ramanathan, V. and Meywerk, J.: Regional aerosol distribution and its long-range transport over the Indian Ocean, J. Geophys. Res. Atmos., 105(D2), 2029–2043, doi:10.1029/1999JD900414, 2000.

Rajeevan, M. and Srinivasan, J.: Net Cloud Radiative Forcing at the Top of the Atmosphere in the Asian Monsoon Region, J. Clim., 13(3), 650–657, doi:10.1175/1520-0442(2000)013<0650:NCRFAT>2.0.CO;2, 2000.

Ramanathan, V., Crutzen, P.J., Coakley, J., Dickerson, R., Heymsfield, A., Kiehl, J., Kley, D., Krishnamurti, T.N., Kuettner, J., Lelieveld, J. and Mitra, A. P.: Indian Ocean Experiment (INDOEX) White Paper, C4 Publ, 143, 1995.

Ramanathan, V. and Ramana, M. V.: Persistent, Widespread, and Strongly Absorbing Haze Over the Himalayan Foothills and the Indo-Gangetic Plains, Pure Appl. Geophys., 162(8–9), 1609–1626, doi:10.1007/s00024-005-2685-8, 2005.

Ramanathan, V., Crutzen, P. J., Kiehl, J. T. and Rosenfeld, D.: Aerosols, Climate, and the Hydrological Cycle, Science (80-. )., 294(5549), 2119–2124, doi:10.1126/science.1064034, 2001.

Randles, C. A., da Silva, A. M., Buchard, V., Colarco, P. R., Darmenov, A., Govindaraju, R., Smirnov, A., Holben, B., Ferrare, R., Hair, J., Shinozuka, Y. and Flynn, C. J.: The MERRA-2 Aerosol Reanalysis, 1980 Onward. Part I: System Description and Data Assimilation Evaluation, J. Clim., 30(17), 6823–6850, doi:10.1175/JCLI-D-16-0609.1, 2017.

Ratnam, M. V., Prasad, P., Roja Raman, M., Ravikiran, V., Bhaskara Rao, S. V., Krishna Murthy, B. V. and Jayaraman, A.: Role of dynamics on the formation and maintenance of the elevated aerosol layer during monsoon

https://doi.org/10.5194/egusphere-2024-3093
Preprint. Discussion started: 27 November 2024


season over south-east peninsular India, Atmos. Environ., 188, 43–49, doi:10.1016/j.atmosenv.2018.06.023, 2018.

Reddy, T. V. R., Mehta, S. K., Ananthavel, A., Ali, S. and Rao, D. N.: Evolution of the planetary boundary layer and its simulation over a tropical coastal station Kattankulathur (12.83°N, 80.04°E), Theor. Appl. Climatol., 146(3–4), 1043–1060, doi:10.1007/s00704-021-03770-2, 2021a.

Reddy, T. V. R., Mehta, S. K., Ananthavel, A., Ali, S., Annamalai, V. and Rao, D. N.: Seasonal characteristics of sea breeze and thermal internal boundary layer over Indian east coast region, Meteorol. Atmos. Phys., 133(2), 217–232, doi:10.1007/s00703-020-00746-1, 2021b.

Sarangi, C., Kanawade, V. P., Tripathi, S. N., Thomas, A. and Ganguly, D.: Aerosol-induced intensification of cooling effect of clouds during Indian summer monsoon, Nat. Commun., 9(1), 3754, doi:10.1038/s41467-018-06015-5, 2018.

SATHEESH, S. and KRISHNAMOORTHY, K.: Radiative effects of natural aerosols: A review, Atmos. Environ., 39(11), 2089–2110, doi:10.1016/j.atmosenv.2004.12.029, 2005.

Savoie, D. L., Prospero, J. M. and Saltzman, E. S.: Non-sea-salt sulfate and nitrate in trade wind aerosols at Barbados: Evidence for long-range transport, J. Geophys. Res. Atmos., 94(D4), 5069–5080, doi:10.1029/JD094iD04p05069, 1989.

Shi, Y., Liu, B., Chen, S., Gong, W., Ma, Y., Zhang, M., Jin, S. and Jin, Y.: Characteristics of aerosol within the nocturnal residual layer and its effects on surface PM2.5 over China, Atmos. Environ., 241, 117841, doi:10.1016/j.atmosenv.2020.117841, 2020.

Stull, R.: An introduction to boundary layer meteorology., 1988.

Su, T., Li, Z., Zheng, Y., Luan, Q. and Guo, J.: Abnormally Shallow Boundary Layer Associated With Severe Air Pollution During the COVID-19 Lockdown in China, Geophys. Res. Lett., 47(20), doi:10.1029/2020GL090041, 2020.

Sun, X., Zhou, Y., Zhao, T., Fu, W., Wang, Z., Shi, C., Zhang, H., Zhang, Y., Yang, Q. and Shu, Z.: Vertical distribution of aerosols and association with atmospheric boundary layer structures during regional aerosol transport over central China, Environ. Pollut., 362, 124967, doi:10.1016/j.envpol.2024.124967, 2024.

Thomas, A., Kanawade, V. P., Sarangi, C. and Srivastava, A. K.: Effect of COVID-19 shutdown on aerosol direct radiative forcing over the Indo-Gangetic Plain outflow region of the Bay of Bengal, Sci. Total Environ., 782, 146918, doi:10.1016/j.scitotenv.2021.146918, 2021.

Tripathi, S. N., Tare, V., Chinnam, N., Srivastava, A. K., Dey, S., Agarwal, A., Kishore, S., Lal, R. B., Manar, M., Kanawade, V. P., Chauhan, S. S. S., Sharma, M., Reddy, R. R., Gopal, K. R., Narasimhulu, K., Reddy, L. S. S., Gupta, S. and Lal, S.: Measurements of atmospheric parameters during Indian Space Research Organization Geosphere Biosphere Programme Land Campaign II at a typical location in the Ganga basin: 1. Physical and optical properties, J. Geophys. Res. Atmos., 111(D23), doi:10.1029/2006JD007278, 2006.

Wang, H., Shi, G. Y., Zhang, X. Y., Gong, S. L., Tan, S. C., Chen, B., Che, H. Z. and Li, T.: Mesoscale modelling study of the interactions between aerosols and PBL meteorology during a haze episode in China Jing–Jin–Ji and its near surrounding region – Part 2: Aerosols' radiative feedback effects, Atmos. Chem. Phys., 15(6), 3277–3287, doi:10.5194/acp-15-3277-2015, 2015.

Wang, H., Li, Z., Lv, Y., Xu, H., Li, K., Li, D., Hou, W., Zheng, F., Wei, Y. and Ge, B.: Observational study of aerosol-induced impact on planetary boundary layer based on lidar and sunphotometer in Beijing, Environ. Pollut., 252, 897–906, doi:10.1016/j.envpol.2019.05.070, 2019a.

Wang, Y., Yao, L., Wang, L., Liu, Z., Ji, D., Tang, G., Zhang, J., Sun, Y., Hu, B. and Xin, J.: Mechanism for the formation of the January 2013 heavy haze pollution episode over central and eastern China, Sci. China Earth Sci., 57(1), 14–25, doi:10.1007/s11430-013-4773-4, 2014.

Wang, Y., Wang, Y., Wang, L., Petäjä, T., Zha, Q., Gong, C., Li, S., Pan, Y., Hu, B., Xin, J. and Kulmala, M.: Increased inorganic aerosol fraction contributes to air pollution and haze in China, Atmos. Chem. Phys., 19(9), 5881–5888, doi:10.5194/acp-19-5881-2019, 2019b.

Wang, Y., Yu, M., Wang, Y., Tang, G., Song, T., Zhou, P., Liu, Z., Hu, B., Ji, D., Wang, L., Zhu, X., Yan, C., Ehn, M., Gao, W., Pan, Y., Xin, J., Sun, Y., Kerminen, V.-M., Kulmala, M. and Petäjä, T.: Rapid formation of

https://doi.org/10.5194/egusphere-2024-3093
Preprint. Discussion started: 27 November 2024


intense haze episodes via aerosol–boundary layer feedback in Beijing, Atmos. Chem. Phys., 20(1), 45–53, doi:10.5194/acp-20-45-2020, 2020.

Wang, Z., Huang, X. and Ding, A.: Dome effect of black carbon and its key influencing factors: a one-dimensional modelling study, Atmos. Chem. Phys., 18(4), 2821–2834, doi:10.5194/acp-18-2821-2018, 2018.

Wilcox, E. M., Thomas, R. M., Praveen, P. S., Pistone, K., Bender, F. A.-M. and Ramanathan, V.: Black carbon solar absorption suppresses turbulence in the atmospheric boundary layer, Proc. Natl. Acad. Sci., 113(42), 11794–11799, doi:10.1073/pnas.1525746113, 2016.

Winker, D. M., Vaughan, M. A., Omar, A., Hu, Y., Powell, K. A., Liu, Z., Hunt, W. H. and Young, S. A.: Overview of the CALIPSO Mission and CALIOP Data Processing Algorithms, J. Atmos. Ocean. Technol., 26(11), 2310–2323, doi:10.1175/2009JTECHA1281.1, 2009.

Xiang, Y., Zhang, T., Liu, J., Lv, L., Dong, Y. and Chen, Z.: Atmosphere boundary layer height and its effect on air pollutants in Beijing during winter heavy pollution, Atmos. Res., 215, 305–316, doi:10.1016/j.atmosres.2018.09.014, 2019.

Xu, T., Song, Y., Liu, M., Cai, X., Zhang, H., Guo, J. and Zhu, T.: Temperature inversions in severe polluted days derived from radiosonde data in North China from 2011 to 2016, Sci. Total Environ., 647, 1011–1020, doi:10.1016/j.scitotenv.2018.08.088, 2019.

Yang, X., Zhao, C., Guo, J. and Wang, Y.: Intensification of aerosol pollution associated with its feedback with surface solar radiation and winds in Beijing, J. Geophys. Res. Atmos., 121(8), 4093–4099, doi:10.1002/2015JD024645, 2016.

Yang, Y., Zheng, Z., Yim, S. Y. L., Roth, M., Ren, G., Gao, Z., Wang, T., Li, Q., Shi, C., Ning, G. and Li, Y.: PM 2.5 Pollution Modulates Wintertime Urban Heat Island Intensity in the Beijing-Tianjin-Hebei Megalopolis, China, Geophys. Res. Lett., 47(1), doi:10.1029/2019GL084288, 2020.

Ye, X., Song, Y., Cai, X. and Zhang, H.: Study on the synoptic flow patterns and boundary layer process of the severe haze events over the North China Plain in January 2013, Atmos. Environ., 124, 129–145, doi:10.1016/j.atmosenv.2015.06.011, 2016.

Young, S. A., Vaughan, M. A., Kuehn, R. E. and Winker, D. M.: The retrieval of profiles of particulate extinction from Cloud-Aerosol Lidar and Infrared Pathfinder Satellite Observations (CALIPSO) data: Uncertainty and error sensitivity analyses, J. Atmos. Ocean. Technol., 30(3), 395–428, doi:10.1175/JTECH-D-12-00046.1, 2013.

Yu, C., Zhao, T., Bai, Y., Zhang, L., Kong, S., Yu, X., He, J., Cui, C., Yang, J., You, Y., Ma, G., Wu, M. and Chang, J.: Heavy air pollution with a unique “non-stagnant” atmospheric boundary layer in the Yangtze River middle basin aggravated by regional transport of PM<sub>2.5</sub> over China, Atmos. Chem. Phys., 20(12), 7217–7230, doi:10.5194/acp-20-7217-2020, 2020.

Yu, H., Kaufman, Y. J., Chin, M., Feingold, G., Remer, L. A., Anderson, T. L., Balkanski, Y., Bellouin, N., Boucher, O., Christopher, S., DeCola, P., Kahn, R., Koch, D., Loeb, N., Reddy, M. S., Schulz, M., Takemura, T. and Zhou, M.: A review of measurement-based assessments of the aerosol direct radiative effect and forcing, Atmos. Chem. Phys., 6(3), 613–666, doi:10.5194/acp-6-613-2006, 2006.

Zhang, H., Wang, Y., Hu, J., Ying, Q. and Hu, X.-M.: Relationships between meteorological parameters and criteria air pollutants in three megacities in China, Environ. Res., 140, 242–254, doi:10.1016/j.envres.2015.04.004, 2015.

Zhang, M., Tian, P., Zeng, H., Wang, L., Liang, J., Cao, X. and Zhang, L.: A Comparison of Wintertime Atmospheric Boundary Layer Heights Determined by Tethered Balloon Soundings and Lidar at the Site of SACOL, Remote Sens., 13(9), 1781, doi:10.3390/rs13091781, 2021a.

Zhang, Y., Zhang, Y., Yu, C. and Yi, F.: Evolution of Aerosols in the Atmospheric Boundary Layer and Elevated Layers during a Severe, Persistent Haze Episode in a Central China Megacity, Atmosphere (Basel)., 12(2), 152, doi:10.3390/atmos12020152, 2021b.

Zhao, D., Xin, J., Gong, C., Quan, J., Liu, G., Zhao, W., Wang, Y., Liu, Z. and Song, T.: The formation mechanism of air pollution episodes in Beijing city: Insights into the measured feedback between aerosol radiative forcing and the atmospheric boundary layer stability, Sci. Total Environ., 692, 371–381, doi:10.1016/j.scitotenv.2019.07.255, 2019.

https://doi.org/10.5194/egusphere-2024-3093
Preprint. Discussion started: 27 November 2024


703 Zhao, J., Du, W., Zhang, Y., Wang, Q., Chen, C., Xu, W., Han, T., Wang, Y., Fu, P., Wang, Z., Li, Z. and Sun,
704 Y.: Insights into aerosol chemistry during the 2015 China Victory Day parade: results from simultaneous
705 measurements at ground level and 260 m in Beijing, Atmos. Chem. Phys., 17(4), 3215–3232, doi:10.5194/acp-
706 17-3215-2017, 2017.

707 Zou, J., Sun, J., Ding, A., Wang, M., Guo, W. and Fu, C.: Observation-based estimation of aerosol-induced
708 reduction of planetary boundary layer height, Adv. Atmos. Sci., 34(9), 1057–1068, doi:10.1007/s00376-016-
709 6259-8, 2017.

710